The Society of Materials Science, Japan

Materials Science Research International, Vol.8, No.3 pp.151-155 (2002)

General paper

Comparing Damage in CFRP Laminates due to Soft Body and Hard Body Impacts

Seung-Min JANG*, Tadaharu ADACHI*, Akihiko YAMAJI*and Joong-Suk KOOK**
* *Department of Mechanical Sciences and Engineering, Tokyo Institute of Technology, 2-12-1, O-okayama, Meguro-ku, Tokyo, 152-8552, Japan*
** *Department of Mechanical Engineering, Daebul University, 72, Samho-ri, Samho-myeun, Youngam-gun, Chonnam, 526-702, Korea*

Abstract: We investigated the damage characteristics in carbon fiber reinforced plastics (CFRP) laminates impacted by soft body and hard body projectiles launched by an air gun. Three kinds of silicone rubber were used as soft body projectiles to investigate the damage resulting from soft body impact that includes material non-linearity and large deformation. Plastic and metallic materials were used as hard body projectiles. From the C-scan images obtained with a scanning acoustic microscope after the tests, we found that the damage mechanism of CFRP laminates in the soft body and hard body impacts was the same. The maximum impact force for each projectile was computed based on the energy balance model and the fundamental hydrodynamics. From this analysis, we found that there is a critical impact force for the delamination initiation and that it is independent of the material properties of the projectiles.

Key words: *Composite Material, Carbon Fiber Reinforced Plastics, Delamination, Impact Damage*

1. INTRODUCTION

Carbon fiber reinforced plastics (CFRP)-laminated composites have been used extensively in many industrial applications due to their good mechanical properties, such as high specific strength and high specific elastic modulus, however, susceptibility to impact damage remains an issue of concern. The damage in CFRP laminates caused by impact includes delamination at interfaces, fiber breakage, and matrix cracking. Such damage may significantly reduce the strength and stiffness of CFRP-laminated composites. Preventing delamination in particular is important to preventing the reduction of compressive strength resulting from an impact. Several studies have addressed the problem of delamination in CFRP laminates under impact conditions [1, 2].

When an aircraft is struck in flight by a bird, which is called a bird strike, the damage to the aircraft can be disastrous, and sometimes fatal. The amount of damage incurred is severe, even if a small bird hits a large aircraft. Thus, in aeronautical engine design, designing jet engine fan blades made of polymer matrix composites so that they are capable of withstanding a bird strike is vital of critical importance. A hard body made of plastic or metallic materials undergoes elastic deformation or some plastic deformation during the impact. However, a soft body impact, such as a bird strike, is a very complicated problem because of the dynamic interaction between the soft body and the mechanical structure, material non-linearity, and large deformations.

Fan [3] conducted a soft body impact test on an aircraft windshield using a mixture of gelatin and water. He measured the pressure applied during the impact by using a piezoelectric sensor and the Hugoniot pressure obtained under the assumption that a soft body projectile could be modeled as a fluid. Ruiz et al. [4] also reported on a bird strike test in which a mixture of gelatin and water was used to simulate a bird strike. Martin [5] conducted nonlinear finite element analysis of soft body impact by using fluid FE formulation. Morita et al. [6] reported that the impact resistance of a composite impacted by a soft body and a hard body was related to the ratio of the damage area to the impact energy. However, the problems of composite materials with respect to soft body impacts, such as a bird strike, are rarely investigated. Furthermore, the effect of soft body properties on the impact damage has not been analyzed yet.

In this paper, we report the results of an investigation of the damage resistance characteristics of CFRP laminates impacted by soft body and hard body projectiles. The projectiles were launched from an air gun and impacted upon CFRP laminates. To compare the effects of the material properties of a soft body projectile on the impact damage, three kinds of silicone rubber were used as the soft body projectiles. Also, impact tests using hard body projectiles made of plastic and metallic materials were carried out and the results were compared with those for the soft body impact tests. After the tests, the delamination initiation in the CFRP laminates was examined in terms of the impact energy and impact force.

2. EXPERIMENTAL PROCEDURE

2.1. CFRP Laminates and Projectiles

The CFRP laminates were fabricated from carbon/epoxy prepreg (Toray, P3051S-22, T700S/#2500). The stacking sequence of each laminate was $[0°_4/\,90°_8/\,0°_4]$. The CFRP laminates were 200 mm long, 100 mm wide, and 3.7 mm thick. Tensile tests of the unidirectional laminates were carried out to characterize their elastic properties by using a universal test machine (Instron 8501). The results were as follows:

Received January 16, 2001
Accepted August 1, 2002

NII-Electronic Library Service

The Society of Materials Science, Japan

Table 1. Mechanical properties of materials.

Type	Projectiles	Material	Longitudinal Modulus [GPa]	Poisson's Ratio	Density [kg/m^3]	Elongation (%)	Mass [g]
Hard Body Material	H1	Aluminum Alloy (JIS A2024)	72.4	0.35	2780	15	1.67
	H2	Epoxy Resin (Bisphenol A)	3.72	0.4	1265	3	0.76
Soft Body Material	S1	Silicone Rubber (KE1402*)	0.14	0.47	1265	400	0.73
	S2	Silicone Rubber (KE112*)	0.69	0.48	1498	120	0.90
	S3	Silicone Rubber (KE26*)	1.28	0.47	1500	70	0.90

* Shin-Etsu Chemical Co., LTD.

$$E_L=114 \text{ GPa}, E_T=8.3 \text{ GPa}, G_{LT}=4.1 \text{ GPa}, \nu_{LT}=0.32$$

where E and G are the longitudinal and transverse moduli, and the subscripts L and T denote, respectively, the longitudinal and transverse-to-the-fiber directions.

Each projectile was 10 mm long, had a diameter of 10 mm, and was rounded with a tip, 12.7 mm in diameter. In general, a largely deformed material under low load is called as a soft material. In this paper, we define a material with low elastic modulus and high elongation as the soft body material. Then, we used three kinds of silicone rubber as the soft body materials and an aluminum alloy and an epoxy resin as the hard body materials. The mechanical properties of materials used as the projectiles are shown in Table 1.

2.2. Impact Test

The impact test apparatus is shown in Fig. 1. The CFRP laminates were simply supported at both ends by two steel circular bars and mounted in front of the air gun. The projectiles expelled from the air gun collided with the center of the CFRP laminates. The impact velocity of each projectile was determined based on the time obtained when the projectile crossed two He-Ne laser beams near the gun muzzle. The impact velocity ranged from 35 m/s to 300 m/s in this experiment.

The impact energy was defined as the kinetic energy of the projectiles just before the collision. White oil paint was used to paint the impacted side of the CFRP laminates before the test to measure the contact area of the projectiles.

After the impact, we observed the damage in the projectiles and the delaminations at the interfaces in the CFRP laminates by using a scanning acoustic microscope (SAM) (Hitachi, AT-5000) having a 10-MHz acoustic lens.

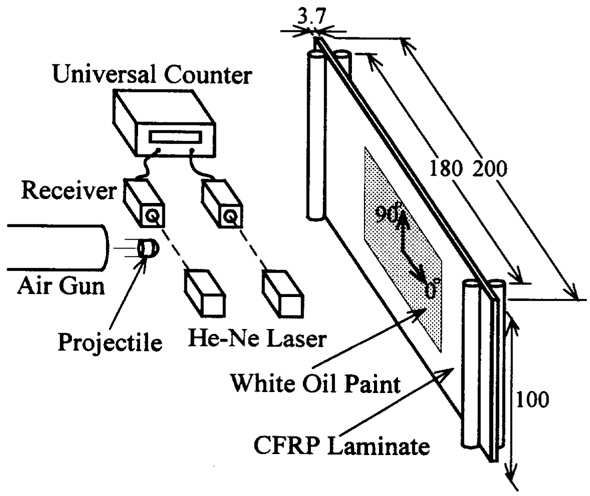

Fig. 1. Experimental apparatus.

3. EXPERIMENTAL RESULTS

3.1. Projectiles after Impact

Figure 2 shows the typical damage to the soft body and hard body projectiles after the impact. In the 'H1' projectile under an impact velocity of more than 120 m/s, there was only a small plastic deformation near the tip and the 'H2' projectile was not damaged at all. In contrast, all the soft body projectiles broke apart in the experiment under the impact velocities ranging from 200

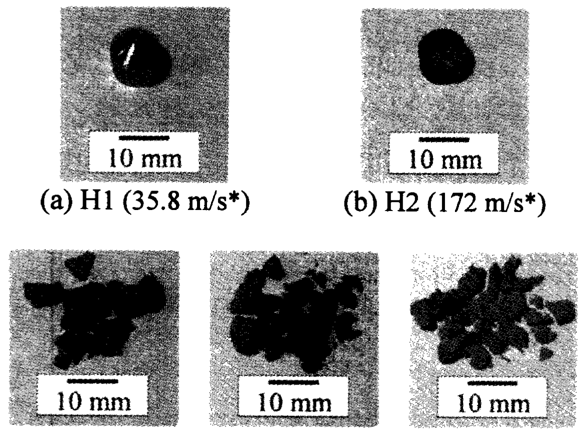

(a) H1 (35.8 m/s*) (b) H2 (172 m/s*) (c) S1 (300 m/s*) (d) S2 (299 m/s*) (e) S3 (299 m/s*)

Fig. 2. Projectile after impact.
*Impact velocity

NII-Electronic Library Service

The Society of Materials Science, Japan

m/s to 300 m/s. Fragments of the soft body projectiles were scattered all over as a result of the collision. After the impact, the size of the scattered fragments was measured. As shown in Fig. 2, the fragments of 'S3' were smaller than those of 'S1' and 'S2'.

3.2. Contact Area

After the impact, we measured the contact area of the projectiles on the CFRP laminates determined from the area where the white oil paint had peeled off. The contact area was approximately circular for each projectile. The relationship between the contact area and the impact energy is shown in Fig. 3. The contact area was increased as the impact energy increased for each projectile. While the maximum contact area produced by each hard body projectile was about half the sectional area of the projectile, the maximum contact area produced by each soft body projectile was three times the sectional area, regardless of the kind of rubber. However, the soft body impacts below the impact energy of 21.6 J did not generate any damage in the CFRP laminates.

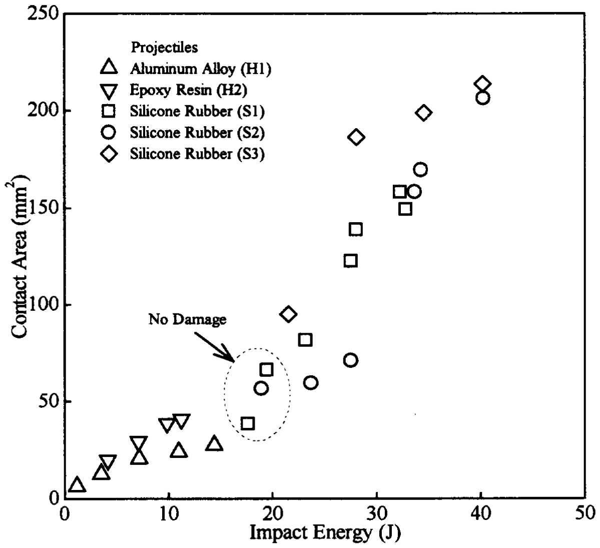

Fig. 3. Relationship between contact area and impact energy.

3.3. CFRP Laminates after Impact

The damaged CFRP laminates had a remarkable matrix cracking oriented in the direction of the fiber on the backside of the impact. The CFRP laminates impacted by the hard body projectiles had distinct indentation marks at the impact point [7]. However, the CFRP laminates impacted by the soft body projectiles had no indentation marks.

Figure 4 shows C-scan images of the delamination at the upper and lower interfaces in the CFRP laminates after the impact observed by the SAM. The delamination area is in the shape of a peanut, which is well known as a typical pattern of impact damage [1]. The shapes of the delamination areas produced by the hard body projectiles were roughly similar to those produced by the soft body projectiles. Thus, we found that the impact damage pattern is essentially independent of the material properties of the projectiles [8].

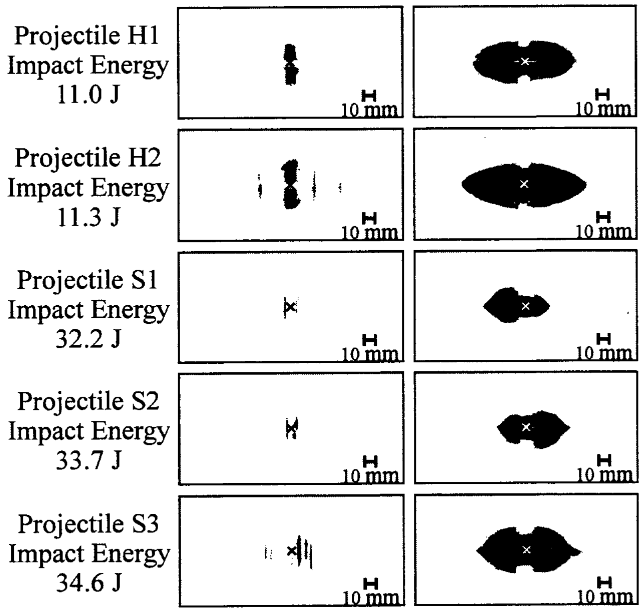

(a) Upper Interface (b) Lower Interface
(X: Impact Point)

Fig. 4. C-scan images at interfaces.

4. DISCUSSION

4.1. Impact Energy

The total delamination area determined by using the SAM was used to quantify the impact damage. The total delamination area is defined as the sum of delamination areas at the upper and lower interfaces.

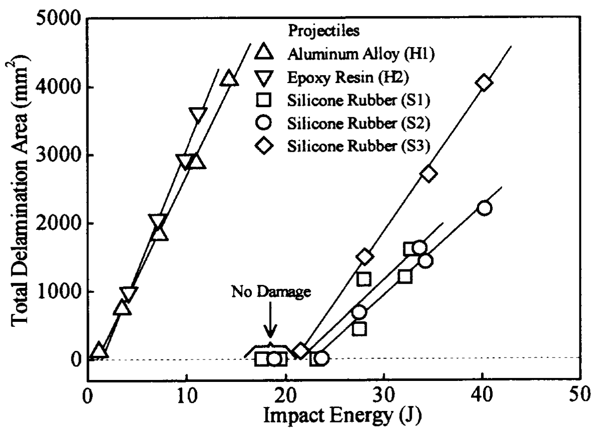

Fig. 5. Total delamination area vs. impact energy.

The relationship between the total delamination area and the impact energy is shown in Fig.5. This relationship is an important parameter characterizing the impact resistance [1, 2, 8]. The delamination area for every projectile was approximately linear to the impact energy, even though the data for the soft body projectiles was a little scattered. The solid line is the least square fitted

NII-Electronic Library Service

The Society of Materials Science, Japan

line. Figure 5 shows that the slopes (DA/IE) of the solid lines for the 'H1', 'H2', and 'S3' projectiles were approximately the same. The slopes for 'S1' and 'S2' are smaller than the others. It is considered that a part of the impact energy was dissipated by the fracture of 'S1' and 'S2' projectiles during the collision. Because the slope denotes the propagation energy of delamination for a unit area, it is related to the reciprocal of the interlaminar fracture toughness. And the dynamic effects must be considered according to the increase in the impact velocity. A ballistic velocity impact induces a localized fracture and perforation at the contact point with no deflection of the CFRP laminate. The delamination area is then the same irrespective of the impact velocity, the CFRP laminate size, and the boundary condition [9]. However, in this experiment, there was no perforation and the delamination area was increased as the impact velocity increased. Also, Vlot [10] proved that the central deflection-energy curve is almost the same for an impact at velocities in the order of 10 m/s and 100 m/s under the same low velocity deformation mode. Thus, the dynamic interlaminar fracture toughness due to the dynamic effects, such as strain rate, was neglected in this experiment [11].

The main difference in the results for the soft body and hard body projectiles was the critical energy that initiated the impact damage in the CFRP laminates. The critical energies in the soft body projectile impacts were much higher than those in the hard body projectile impacts. Therefore it is apparent that initiation of delamination is not governed by impact energy alone.

4.2. Impact Force

We calculated the impact force to investigate the relationship between the initiation of delamination and the impact force because the initiation of delamination and the impact energy did not show any relation in the results obtained experimentally. Because the hard body projectiles had elastic and small plastic deformations as a result of collision in the experiment, we assumed that the hard body projectiles were elastic in the analysis. In contrast, each soft projectile was smashed by the collision, and the fragments of the projectiles were scattered as if they were a fluid. We thus used the approximation of a perfect liquid in the computation of the impact force of the soft body projectiles [12, 13].

First, the energy balance model [14, 15, 16] was widely used to calculate the impact force of each hard body projectile. The basic assumption in this analysis is that the initial kinetic energy of the projectiles is transferred into the CFRP laminates during the impact because the energy absorbed by the system during an impact is of negligibly small quantities in comparison with the energies used in the indentation and the deflection of CFRP laminates [17]. Thus, the maximum impact force and the maximum deflection of the CFRP laminates occur simultaneously when the velocity of the projectiles is zero. We investigated the local deformation at the contact point between the CFRP laminates and the projectiles. The energy losses due to vibration, heat, sound, etc., were neglected. The energy balance equation [1, 14] can be written as

$$\frac{1}{2}M_H V_H^2 = \int_0^{w_{max}} P dw + \int_0^{\alpha_{max}} P d\alpha, \quad (1)$$

where P is the impact force the CFRP laminates received during the impact, M_H and V_H are, respectively, the mass and the impact velocity of the hard body projectile, and w and α are, respectively, the deflection of the CFRP laminates at the impact point and the local deformation of the CFRP laminates created by the contact with the projectiles.

The deflection of the CFRP laminates is related to the impact force, given as

$$P = k \cdot w, \quad (2)$$

where k is the linear stiffness of the CFRP laminates calculated according to the classical CFRP laminated beam theory. The contact force is given by Hertz's contact theory.

$$P = n \cdot \alpha^{3/2}, \quad (3)$$

where n is the Herzian contact stiffness. Sun et al. [18] suggested a modified formulation of the contact stiffness between a spherically rounded projectile and a CFRP laminated plate as follows:

$$n = \frac{4}{3}\sqrt{r_H} \cdot \frac{1}{\frac{1-\nu_H^2}{E_H} + \frac{1}{E_T}}, \quad (4)$$

where E_T is Young's modulus of the transverse direction to the fibers of CFRP laminates, r_H, ν_H, and E_H are, respectively, the curvature radius at the tip, the Poisson's ratio, and Young's modulus of the hard body projectile.

By substituting Eqs. (2) and (3) into Eq. (1) and integrating the equation, we obtain the following equation:

$$\frac{1}{2}M_H {V_H}^2 = \frac{1}{2}\frac{{P^2}_{max}}{k} + \frac{2}{5}\frac{{P^{5/3}}_{max}}{n^{2/3}}. \quad (5)$$

Therefore, the maximum impact force of the hard body projectiles, P_{max}, can be obtained from the numerical analysis of Eq. (5).

Equation (5) cannot be used to analyze the collision of the soft body projectiles because the contact deformation of these projectiles is not localized at the impact point due to Hertz's theory. That is, the momentum of the soft body projectiles disappears at the impact point because of the assumption of a perfect liquid. Then the impact force of the soft body projectiles can be calculated based on the fundamental hydrodynamics [12].

$$P = \rho_S \cdot A_S \cdot (V_S(t) - \dot{w}(t)),^2 \quad (6)$$

NII-Electronic Library Service

The Society of Materials Science, Japan

where ρ_S and A_S are the density and the cross sectional area of the soft body projectile, respectively. $V_S(t)$ and $\dot{w}(t)$ are the velocity of the soft body projectile and the deflection rate of the CFRP laminate during the impact. The pressure waves originating at the impact location and propagating through the soft body produce the pressure peaks, the so-called "Hugoniot pressures". After that, the maximum pressure at the beginning of the impact is decreased by the dispersion of the fractured projectile [19]. Thus, the impact force becomes maximum just after the collision. Therefore, the maximum impact force, P_{max}, at $\dot{w}(t) = 0$, can be written as

$$P = \rho_S \cdot A_S \cdot {V_{SI}}^2. \tag{7}$$

where V_{SI} is the velocity of the soft body projectile just before the impact on the CFRP laminates.

The relations between the total delamination area and the maximum force are shown in Fig 6. The solid line is fitted to the analyzed results for each projectile. Although the slopes of the lines are different, Figure 6 clearly shows that there is a distinct initial value of the maximum impact force that induces the delamination of the CFRP laminates regardless of the projectile material. This means that the delamination initiation is governed by the critical value of the maximum impact force.

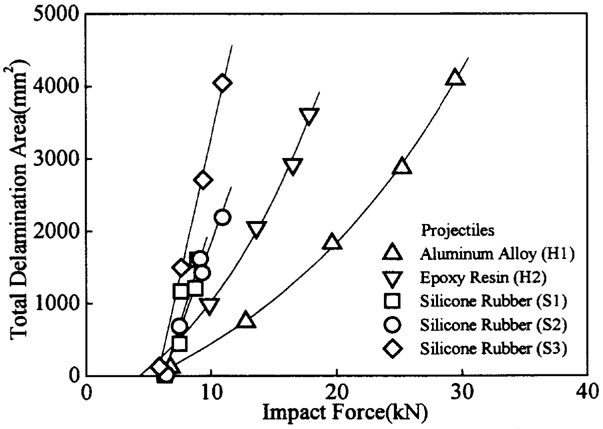

Fig. 6. Total delamination area vs. maximum impact force.

5. CONCLUSION

We investigated the damage characteristics of CFRP laminates impacted by soft body and hard body projectiles. The delamination patterns measured by using a scanning acoustic microscope showed no difference between the soft body impacts and the hard body impacts. These results mean that the mechanism of damaging CFRP laminates in a soft body and a hard body is the same. The relationship between the delamination area (DA) and the impact energy (IE) was linear, and the ratio of DA/IE, which indicated the propagation energy of delamination in the CFRP laminates during impact, was the same in both soft body and hard body impacts, but when a soft body having high elongation was impacted, the ratio of DA/IE was a little low because a part of the impact energy was dissipated by the fracturing of soft body projectiles during the collision. We also found that there is a critical impact force for the initiation of delamination, and that it is independent of the material properties of projectiles.

REFERENCES

1. S. Abrate, Applied Mechanics Review, **44** (1991) 155.
2. S. Abrate, Applied Mechanics Review, **47** (1994) 517.
3. H.T. Fan, Waves and Fracture, AMD-Vol.205 (ed. by R.C. Batra, A.K. Mal and G.P. MacSithigh), ASME, (1995) 43.
4. C. Ruiz and R. Duffin, Proc 11th Int. Conf. Experimental Mechanics, (ed. by I.M. Allison), A.A.Balkema (1998) 143.
5. N.F. Martin Jr., Journal of Propulsion & Power, **6** (1990) 445.
6. H. Morita, and P.H.W. Tsang, Journal of Reinforced Plastics & Composites, **16** (1997) 1330.
7. T. Adachi, M. Okazaki, S. Ujihashi and H. Matsumoto, JSME International Journal, **38A** (1995) 370.
8. H. Morita, T. Adachi, Y. Tateishi and H. Matsumoto, Journal of Reinforced Plastics & Composites, **16** (1997) 131.
9. W.J. Cantwell, J. Morton, Composites, **20** (1989) 545.
10. A. Vlot, International Journal of Impact Engineering, **18** (1996) 291.
11. T. Adachi, M. Arai, N. Sakabe and H. Matsumoto, JSME International Journal, **43A** (2000) 179.
12. T. Adachi, S. Yamamura, M. Arai and H. Matsumoto, Impact Response of Materials and Structures, (ed. by V.P.M. Shim, S. Tanimura and C.T. Lim), Oxford (1999) 467.
13. J.L. Preston Jr. and T.S. Cook, ASTM STP 568 (1975) 49.
14. W.C. Jackson and C.C. Poe Jr., Journal of Composites Technology & Research, **15** (1993) 282.
15. S. Abrate, Composite Structures, **51** (2001) 129.
16. H.M. Wen, T.Y. Reddy, S.R. Reid and P.D. Solden, Key Engineering Materials, **141-143** (1998) 501.
17. D. Delfosse, A. Poursartip, Composites, **28A** (1997) 647.
18. C.T. Sun and S.H. Yang, ASTM STP 787 (ed. by I.M. Daniel), (1982) 425.
19. J.S. Wilbeck, Journal of Engineering for Power, **130** (1981) 725.

NII-Electronic Library Service